CHAPTER 178

DYNAMICS OF A LONGITUDINALLY STRATIFIED ESTUARY

by

Jorg Imberger*

1. Introduction.

A partially stratified estuary is defined as one which possesses a quite definite longitudinal salinity gradient from the mouth to the head of the estuary, but only a very weak vertical or transverse salinity structure. For an estuary to exhibit such characteristics it must possess a source of fresh water near the head of the estuary, sufficient vertical mixing to overcome the potential energy associated with such a fresh water inflow and be very much longer than its width to reduce transverse variations.

If the estuary is very shallow (a few meters) then wind generated turbulence is often sufficient to eliminate most or all the vertical structure. Deeper, or very sheltered, estuaries require additional strong tidal shears to break up the vertical density gradients. However, in both cases the mixing is usually not sufficient to completely homogenize the estuary longitudinally and it is found that these estuaries display a near linear salinity gradient along the principle axis of the estuary throughout most of the spring and summer months.

Such a density gradient drives a gravitational circulation within the estuary which leads to a net transport of salt from the sea mouth to the head of the estuary. Two dimensional theories (see for instance Rattray and Mitsuda (1974)) have been established, but in general these greatly underestimate the longitudinal transport found in such estuaries and three dimensional circulation effects must be considered.

Fischer (1972) was the first to recognise this fact and he carried out a first order analysis which pointed to a greatly increased longitudinal dispersion. However, Fischer (1972) carried out his analysis only to first order, not explaining how the transverse pressure field, set up by the first order velocity field convecting the longitudinal density gradient, is balanced. It is the purpose of this paper to give a rigorous foundation to Fischer's (1972) hypothesis that it is the transverse variations in velocity which yield the greatest contribution to any longitudinal transport of the density or any passive pollutant. Furthermore, the presented theory is applied to a local Western Australian estuary which is ideally suited for such a comparison complying strictly to the assumptions of the theory.

In order to facilitate the theoretical work the experimental apparatus described in Imberger (1974) was modified and used to visualize the flow. An insulated, completely enclosed perspex tank possessing a triangular section and containing water was heated

*Senior Lecturer, Departments of Mathematics and Mechanical Engineering, University of Western Australia, Nedlands, 6009, W.A.

at one end and cooled at the other. The dimensions of the tank were 2.58 meters long, 0.45 meters wide and 0.05 meters deep at one side and of zero depth at the other. The flow was visualized by the thymol blue technique and the temperature was measured with small thermistors.

The motion was in general difficult to quantify because of its three dimensional nature. However, two features were common to all the motions observed. Firstly, in the central sections of the tank, away from the end walls, the motion was confined to vertical planes, parallel to the longitudinal axis. The warm fluid at the top flowed towards the cold end and the colder undercurrent flowed towards the warmer end wall. In the shallow sections the net flow was towards the cold end wall, while in the deeper parts the net flow was towards the warmer end wall. Secondly, the temperature structure was approximately independent of the transverse coordinate and dependent only on the distance along the longitudinal axis and the depth below the upper surface.

Hence, the experiments indicated that the dominant force balance of such a flow is

$$\varepsilon_z \frac{\partial^3 u}{\partial z^3} + \frac{g}{\rho_0}\frac{\partial \rho}{\partial x} = 0, \text{ where } u \text{ is}$$

the longitudinal velocity, ρ is the density, ρ_0 is a reference density, ε_z is the vertical mixing coefficient for vorticity, g is the acceleration due to gravity and x and z are the horizontal and vertical coordinates. This balance yields a scale for the velocity u in terms of the longitudinal density gradient $\frac{\partial \rho}{\partial z}$ and a non-dimensionalizing of the full flow equations, based on this force balance, is shown in section 2 to admit a consistent perturbation solution very similar to that described by Cormack, Leal and Imberger (1974).

2. Gravitational circulation in a triangular shaped basin

Consider half of an idealized estuary as shown in figure 1, filled with water which is kept in motion by a longitudinally applied buoyancy flux. The basin is assumed to possess a cover in contact with the water. This is not an essential assumption and a non conducting free surface could be treated just as easily. The result with regard to the final mass transport is quite insensitive to this boundary condition, yet the pressure field is simplified reducing the algebra somewhat. All sides and top surfaces are considered to be non-conducting and the emphasis will be on investigating the flow in the central sections of the basin where the flow is essentially in the vertical plane. The end regions where the flow is turned are neglected.

From the experiments described in the introduction the following seales are apparent;

$$\text{Density: } \frac{\rho - \rho_0}{\rho_0} = O(\Delta\rho),$$

$$\text{Horizontal length: } x = O(L)$$

$$\text{Transverse length: } y = O(B)$$

$$\text{Vertical length: } z = O(H)$$

$$\text{Horizontal velocity: } u = O\left(\frac{Gr\ \varepsilon_z}{L}\right)$$

$$\text{Transverse velocity: } v = O\left(\frac{B\ Gr\ \varepsilon_z}{L^2}\right)$$

$$\text{Vertical velocity: } w = O\left(\frac{H\ Gr\ \varepsilon_2}{L^2}\right),$$

where $\Delta\rho$ is the applied density variation, Gr is the effective Grasshoff number $g\Delta\rho H^3/\varepsilon_z^2$, ε_z the vertical vorticity diffusion coefficient assumed to be constant and g is the acceleration due to gravity.

This suggests introducing the non-dimensional variables:

$$u^* = \frac{u}{\frac{Gr\ \varepsilon_z}{L}} \ ; \quad v^* = \frac{v}{\frac{B\ Gr\ \varepsilon_z}{L^2}} \ ; \quad w^* = \frac{w}{\frac{H\ Gr\ \varepsilon_z}{L^2}} \ ; \quad p^* = \frac{p}{\frac{\varepsilon_z^2 \rho_0 Gr}{H^2}}$$

$$\theta^* = -\frac{\rho - \rho_0}{\rho_0 \Delta\rho}; \quad x^* = \frac{x}{L} \ ; \quad y^* = \frac{y}{B} \ ; \quad z^* = \frac{z}{H}$$

Interest here centres on very shallow, long estuaries with aspect ratios

$$A_1 = \frac{H}{L} \ , \quad A_2 = \frac{H}{B} \ \text{ and } \ A_3 = \frac{B}{L}$$

all being very small. However, for a perturbation scheme to be applicable, these must be ordered. The most realistic limit is obtained by setting

$$A_2 = A, \quad A_1 = \alpha A^2 \ \text{ and } \ A_3 = \alpha A \ \text{ where}$$

α is the ratio B^2/LH as $H \to 0$, $L \to \infty$. The Bousinesque approximation to the full equations of motion for the mean components of the velocity may thus be written:

$$\alpha^2A^4Gr(uu_x + vu_y + wu_z) = -p_x + \lambda\alpha^2u_{xx} + \lambda A^2u_{yy} + u_{zz} , \qquad (1)$$

$$\alpha^4A^6Gr(uv_x + vv_y + wv_z) = -p_y + \alpha^4\lambda A^6v_{xx} + \alpha^2\lambda A^4v_{yy} + \alpha^2A^2v_{zz} , \qquad (2)$$

$$\alpha^4A^8Gr(uw_x + vw_y + ww_z) = -p_z + \theta + \alpha^4\lambda A^8w_{xx} + \alpha\lambda^2A^6w_{yy} + \alpha^2A^4w_{zz}, \qquad (3)$$

$$\alpha^2A^4GrPr(u\theta_x + v\theta_y + w\theta_z) = \lambda\alpha^2A^4\theta_{xx} + \lambda^2A^2\theta_{yy} + \theta_{zz} , \qquad (4)$$

$$u_x + w_y + w_z = 0 , \qquad (5)$$

where $\lambda = \dfrac{\varepsilon_y}{\varepsilon_z} = \dfrac{\varepsilon_x}{\varepsilon_z}$, $Pr = \dfrac{\varepsilon_z}{\kappa_z}$ and all asterisks have been dropped.

The scaling has captured the dominant physical processes and an appropriate solution may be sought in the form,

$$\phi(\underset{\sim}{x} \; ; \; A) = \phi_0 + A^2 \; \phi_2 + A^4 \; \phi_4 + \dots , \qquad (6)$$

where ϕ represents the variables u, v, w and p.

Substituting this expansion into the above and expanding terms leads to:

$O(A^0)$:

$$p_{0_x} - u_{0_{zz}} = 0 , \qquad (7)$$

$$p_{0_y} = 0 , \qquad (8)$$

$$p_{0_z} - \theta_0 = 0 , \qquad (9)$$

$$\theta_{0_{zz}} = 0 , \qquad (10)$$

$$u_{0_x} + v_{0_y} + w_{0_z} = 0 , \qquad (11)$$

$O(A^2)$:

$$p_{2_x} - u_{2_{zz}} = \lambda u_{0_{yy}} , \qquad (12)$$

$$p_{2_y} = \alpha^2 v_{0_{zz}} ,$$

$$p_{2_z} - \theta_2 = 0 ,$$

$$\theta_{2_{zz}} = -\lambda\theta_{0_{yy}} ,$$

$$u_{2_x} + v_{2_y} + w_{2_z} = 0 ,$$

$$O(A^4): \quad p_{4_x} - u_{4_{zz}} = -Gr\alpha^2(u_0 u_{0_x} + v_0 u_{0_y} + w_0 u_{0_z}) + \lambda\alpha^2 u_{0_{xx}} + \lambda u_{2_{yy}} , \tag{17}$$

$$p_{4_y} = \lambda\alpha^2 v_{0_{yy}} + \alpha^2 v_{2_{zz}} , \tag{18}$$

$$p_{4_z} - \theta_4 = \alpha^2 w_{0_{zz}} , \tag{19}$$

$$\theta_{4_{zz}} = \alpha^2 PrGr(u_0\theta_{0_x} + v_0\theta_{0_y} + w_0\theta_{0_z}) - \lambda\alpha^2\theta_{0_{xx}} - \lambda\theta_{2_{yy}} , \tag{20}$$

$$u_{4_x} + v_{4_y} + w_{4_z} = 0 . \tag{21}$$

The solution to the problem may now be carried out in stages. Consider the zeroth order problem.

Equation (10) implies

$$\theta_0 = f_1(x,y)\ z + f_0(x,y) ,$$

but at $z = 0$, $\theta_{0_z} = 0$ which requires that $f_1 = 0$.
Also equation (9) together with equation (8) prohibit f_0 to be a function of y. Hence

$$f_0 = f_0(x), \tag{22}$$

where f_0 must be determined from higher order equations and the end boundary conditions.

Eliminating the pressure from equations (9) and (7) yields

$$u_{0_{zzz}} = f_{0_x} , \tag{23}$$

which allows u_0 to be determined

$$u_0(y,z) = \frac{h^3}{12} f_{0_x}\left(\frac{2z^3}{h^3} + \frac{3z^2}{h^2} + \frac{z}{h}\right) - \frac{6U_0}{h}\left(\frac{z^2}{h^2} + \frac{z}{h}\right), \tag{24}$$

where h is the local depth equal to $-y$ and U_0 is the net volume flux towards the lighter end of the basin. This may be determined from equations (8) and (7) which require

$$u_{0_{zzy}} = 0. \tag{25}$$

The total net flux over the triangular section shall be assumed to be zero, thus substituting equation (24) into equation (25) leads to

$$U_0(y) = \frac{1}{30} \frac{\partial f_0}{\partial x} y^3 \left(1 + \frac{5}{4} y\right) \tag{26}$$

Equation (15) and the no flux boundary at $z = 0$ require that

$$\theta_2 = f_2(x,y), \tag{27}$$

where $f_2(x,y)$ must still be determined.

Integrating equation (20) from $-h$ to zero with respect to z yields

$$-\theta_{4_z}(z = -h) = \alpha^2 \mathrm{PrGr} f_{0_x} U_{0_x} - 2\alpha^2 f_{0_{xx}} h - \lambda\theta_{2_{yy}} h, \tag{28}$$

which is only possible if

$$f_0 = kx\,, \quad \text{where } k \text{ is a}$$

constant - determined by the flow in the end regions. For the two dimensional analogue Cormack, Leal and Imberger(1974)solved the end regions to show that k could itself be expanded in a power series of A. Here k will be taken as experimental data since the three dimensional motion in end regions where the flow turns is far too complex to solve in closed form.

The heat flux $\theta_{4_z}(z = -h)$ is strictly non-zero since

Phillips (1970) type boundary layer always exist at a sloping wall in a stratified fluid. However, the heat flux necessary to drive such a layer at small angles is very small, certainly not an appreciable proportion of the flux convected by U_0 and θ_{4_z} may thus in the first instance be set to zero at $z = -h$. If desired a wall boundary layer could be added with small modifications resulting to the main flow.

Setting $\theta_{2_y}(y = -1) = 0$ and $\theta_2(y = -\frac{4}{5}) = 0$ completely determines the second order temperature field.

$$\theta_2(y) = -\frac{\alpha^2 PrGr\, k^2}{1440\lambda} \quad (3y^5 + 4y^4 + y + 0.1446) \cdot \tag{29}$$

Eliminating the pressure from equations (13) and (14) and substituting equation (29) into the resulting equation yields,

$$v_0(y,z) = -\frac{PrGr\ k^2}{288\alpha^2} \left(\frac{y^4}{4} + \frac{4}{15} y^3 + \frac{1}{60} \right)(2z^3 - 3z^2 y + zy^2) \tag{30}$$

Equation (11) allows a streamfunction $\psi_0(x,y)$ to be defined such that

$$v_0 = \psi_{0_z} \quad \text{and} \quad w = -\psi_{0_y}$$

From equation (30) ψ_0 may thus be determined

$$\psi_0(y,z) = -\frac{PrGr\ k^2}{576\ \alpha^2} z^2 (y - z)^2 \left(\frac{y^4}{4} + \frac{4}{15} y^3 + \frac{1}{60} \right). \tag{31}$$

The flow represented by equation (31) is depicted in figure 2 and it consists of two opposing eddies.

Eliminating the pressure from equations (12) and (14) and substituting for u_0 allows u_2 to be determined.

$$u\ (x,z,y) = \frac{k}{36} (2z^3 - 3z^2 y + 2y^2) + \frac{6U_2(x,y)}{y^3} (z^2 - zy) \tag{32}$$

and U_2 may be determined from equations (12) and (13):

$$U_2(y) = \frac{ky^3}{72} \left(y + \frac{4}{5}\right) \cdot \tag{33}$$

Finally, substituting u_0, θ_0 and θ_2 into equation (20) allows the determination of the 4th order temperature field:

$$\theta_4(z,y) = \frac{\alpha^2 PrGr\ k^2}{24} \left\{ \left(\frac{z^5}{5} - \frac{z^4 y}{2} + \frac{z^3 y^2}{3} - \frac{y^5}{60} \right) + \frac{z^2}{2} \right.$$
$$\left. \left(y + \frac{4}{5}\right)(z - y)^2 \right\}, \tag{34}$$

where the integration constant has been chosen so that $\theta_4 = 0$, $z = \frac{1}{2}y$ and $y = -\frac{4}{5}$.

The quantities so far determined allow the mass transfer to be computed correct to $O(A^4)$. Higher order terms may however easily be derived.

3. Longitudinal mass transfer

The convective mass transfer in the x direction is given by

$$q = \int_{-B}^{0}\int_{-h}^{0} \theta u \, dz \, dy = \frac{HBGr\varepsilon_z \Delta\rho}{L} \int_{-1}^{0}\int_{y}^{0} \theta^* u^* dz^* dy^*$$

$$= \frac{HBGr\varepsilon_z \Delta\rho}{L} \int_{-1}^{0}\int_{y}^{0} \{(\theta^*_2 u^*_0)A^2 + (\theta^*_4 u^*_0 + \theta^*_2 u^*_2)A^4\} \, dz^* dy^* \tag{35}$$

Substituting from section 2 for θ_0, u_0, θ_2, u_2 and θ_4 and carrying out the integration yields

$$q = - HBD \, k^3 , \tag{36}$$

where

$$D = \frac{\kappa_z \Delta\rho}{L} \quad \frac{\alpha^2 Pr^2 Gr^2 A^2}{\lambda} \{1.286 \times 10^{-7} + 6.81 \times 10^{-5} A^2 \lambda + \}.$$

So far the flow has been considered steady, but since there is a net flux from the estuary mouth to the head of the estuary the salinity will build up there. In line with Taylor's (1954) argument it will be assumed that the time scale of this change is large compared to the flow establishment time. Furthermore, if it is also assumed (again following Taylor(1954) that the gradients of $f_0(x)_x$ are small enough for the above theory to hold, at least, locally, then a mass balance, averaged across any cross-section yields the relationship

$$\frac{dq}{dx} = - \frac{HB}{2} \frac{\partial\theta_0}{\partial t} . \tag{37}$$

Substituting equation (36) into (37) yields an equation for $\theta_0(x)$

$$\frac{\partial\theta_0}{\partial t} = 6D\left(\frac{d\theta_0}{\partial x}\right)^2 \frac{d^2\theta_0}{dx^2} , \tag{38}$$

which may be viewed to the equivalent to Taylor's (1954) mean diffusion equation, the only difference being that the tracer here is the salinity itself which also drives the motion. The exact anology for the two dimensional flow is discussed in more detail in Imberger (1974).

The exact solution of equation (38) is difficult to obtain for a bounded domain $0 < x < L$. For comparison with experimental work it is sufficient to note that equation (38) admits a self similar valid in the unbounded domain

$$\theta = \theta\left(\frac{x^2}{\sqrt{DE}}\right) , \tag{39}$$

yielding a time scale for salinity adjustments at the end of an enclosed estuary of the order of

$$T = \left(1.3 \times 10^7 \frac{\Delta\rho^2 L^2 \lambda}{\kappa_z Pr^2 Gr^2 A_3^2}\right) . \tag{40}$$

4. Application to the Harvey Estuary

The Harvey estuary situated about 80 km south of Perth is a long, shallow coastal lagoon, behind and parallel with the late Pleistocene dunes. Fig. 3 shows the general bathymetry of the basin and indicates the suitability of the Harvey for testing the above theory. The principle axis of the basis is oriented along the direction of the major wind system which blew consistently from the south with a mean velocity of between 6 and 10 km/hr for most of the study period.

The measurements were initiated in July 1974 when the fresh water inflow for the season was at its maximum. The stations at which the salinity and temperature were measured are indicated on fig. 3 and the actual values recorded are listed in table 1. All measurements were recorded from a small dinghy with a standard induction salinometer.

Figure 4 shows the average salinity plotted against distance from station 140 for the period July to April. The fresh water inflow had ceased almost completely by October 1974. Table 2 shows that the variations with depth are indeed small past station 150 consistent with the assumption of a well stirred lagoon. Table 2 lists the comparison of the experimental findings with those predicted from the above theory. All the assumed values of constants are shown and it is seen that the response time for salinity variations at the southern extreme (station 180 and 190) due to applied changes at Station 140 are predicted quite well. Careful probing of the deepest depressions along the central trough showed evidence of pools of saltier water (usually 1 or $2^{\circ}/oo$ higher) of about 5 to 10 cm thickness underlying the well mixed water above. This indicates that the 1.5 meter depth is on the limit of wind mixing and salt replenishment by salt wedge underflow does take place on the more calm days. It was very difficult to estimate the magnitude of the contribution to the salt transport by this later mechanism as little is known about the entrainment across a density interface under surface waves. However, the lateral extent was no more than 300 meters i.e. 1/10 of the width. Assuming a fully active layer of thickness $h_0 = 5$ cm with a velocity $(\Delta\rho\ gh_0)^{\frac{1}{2}} = 0.02$ m sec^{-1} and a salinity gradient $\Delta\rho/L = 5.5 \times 10^{-8}$ leads to a flux of $O(h_0 b_0 u\theta_x) = 8.75 \times 10^{-9}$ compared to 1.9×10^{-6} m^{2}sec^{-1} for the slow circulation mechanism.

4. Acknowledgement

The author would like to thank Mr. Ron Black, Western Australian Institute of Technology, for helping in the collection of the physical data.

References

Cormack, D.E., Leal, L.G., Imberger, J. 1974
J. Fluid Mech. Vol. 65, pt 2, pp 209 - 229.

Fischer, H.B., 1972
J. Fluid Mech. Vol. 53, pt 4, pp 671 - 687.

Imberger, J. 1974
J. Fluid Mech. Vol. 65, pt 2, pp 247 - 260.

Rattray, M., Mitsuda, E. 1974
Estuarine and Coastal Marine Science, Vol. 2, pp 375 - 394.

Phillips, O.M. 1970
Deep-Sea Res. 17, 435-43 p 244.

Taylor, G.I. 1954
Proc. Roy. Soc. of London 223 pp 446 - 468.

Station Distance km		140 0.00		150 3.35		152 4.90		160 11.05		180 14.20		190 17.80	
Date	Depth	Temp °C	Sal °/oo	Temp °C	Sal °/oo	Temp °C	Sal °/oo	Temp °C	Sal °/oo	Temp °C	Sal °/oo	Temp °C	Sal °/oo
10th July 1974	0.0	13.7	7.0					13.2	5.0			15.0	1.3
	Average	13.7	7.0					13.2	5.0			15.0	1.3
13th Oct 1974	0.00	18.5	13.4	17.6	11.6			17.9	8.9	17.8	7.7		
										17.8	7.6		
	1.00	18.4	14.0	17.6	11.6			17.9	8.9	17.8	7.7		
	1.50	18.2	15.0	16.9	13.6			17.9	8.9	17.8	7.7		
	Average	18.36	14.13	17.3	12.2			17.9	8.9	17.8	7.6		4.8
13th Nov 1974	0.00	22.5	17.0	21.2	13.6	21.2	13.0	22.4	12.4	22.8	11.9	23.2	11.2
	0.50	22.5	17.0	20.0	13.5	20.6	12.8	21.2	12.4	22.2	17.2	21.8	17.2
	1.00	22.0	17.2	19.5	13.6	19.6	13.02	20.5	13.0	21.3	12.6	21.0	12.3
	1.50	21.7	17.6	19.2	14.2	19.6	14.5	20.5	13.0	20.6	12.6	20.6	12.4
	Average	22.1	17.2	19.9	13.7	20.2	13.3	21.15	12.7	21.7	13.5	21.6	12.2
7th Jan 1975	0.00	–	31.6	22.5	30.5			21.3	26.5	21.0	26.5	21.1	26.2
	0.50			22.5	30.5			21.3	26.5	21.0	26.5	21.2	26.3
	1.00			22.5	30.5			21.3	26.5	21.0	26.5	21.2	26.3
	1.50			22.5	30.5			21.3	26.8	21.0	26.5		
	Average		31.6	22.5	30.5			21.3	26.5	21.0	26.5	21.1	26.2
20th Jan 1975	0.00					27.0	31.3	21.8	30.3	21.7	29.6	23.0	29.3
	0.50					21.9	31.5	21.6	30.3	21.5	30.1	22.5	29.3
	1.00					21.3	32.0	21.2	30.4	21.4	30.5	22.4	29.3
	1.50					21.2	32.2	21.1	30.7	21.3	30.5	21.8	29.6
	Average					22.8	31.7	21.4	30.4	21.4	30.1	22.4	29.3
23rd Apr 1975	0.0	18.0	38.1					18.0	37.6			21.0	36.9
	Average	18.0	38.1					18.0	37.6			21.0	36.9

Table 1.

Assumed constants

Length L	$= 18$ km
Depth H	$= 1.5$ m
Half width B	$= 1.5$ km
Aspect ratio A_1	$= 8.3 \times 10^{-5}$
Aspect ratio A_2	$= 10^{-3}$
Aspect ratio A_3	$= 8.3 \times 10^{-2}$
Ratio α	$= 83$
Applied density difference $\Delta\rho/\rho_0$	$= 10^{-2}$
Vertical vorticity exchance coefficient ε_z	$= 10^{-3} m^2 sec^{-1}$
Ratio of horizontal to vertical exchange coefficient λ	$= 80$
Turbulent Prandtl number Pr	$= 1$
Turbulent Grasshoff number Gr	$= 3.7 \times 10^5$
Predicted time response T	$= 34$ days
Observed time response (from fig. 5.2) T	$= 1$-2 months
Predicted magnitude of vertical salinity variations	$O\left(\alpha^2 PrGrk^2 \times 10^{-3} \frac{\Delta\rho}{\rho_0}\right)A^4 = 2.5 \times 10^{-5}$ $^o/oo$
Predicted magnitude of horizontal salinity variation	$O\left(\frac{\alpha^2 PrGrk^2}{\lambda} \frac{\Delta\rho}{\rho_0} A^2 10^{-3}\right) = 0.32$ $^o/oo$
Predicted maximum net flow along principle axis	$Q(y = -1) = 0.03 m^2 sec^{-1}$

Note: The last three quantities were not measurable.

Table 2.

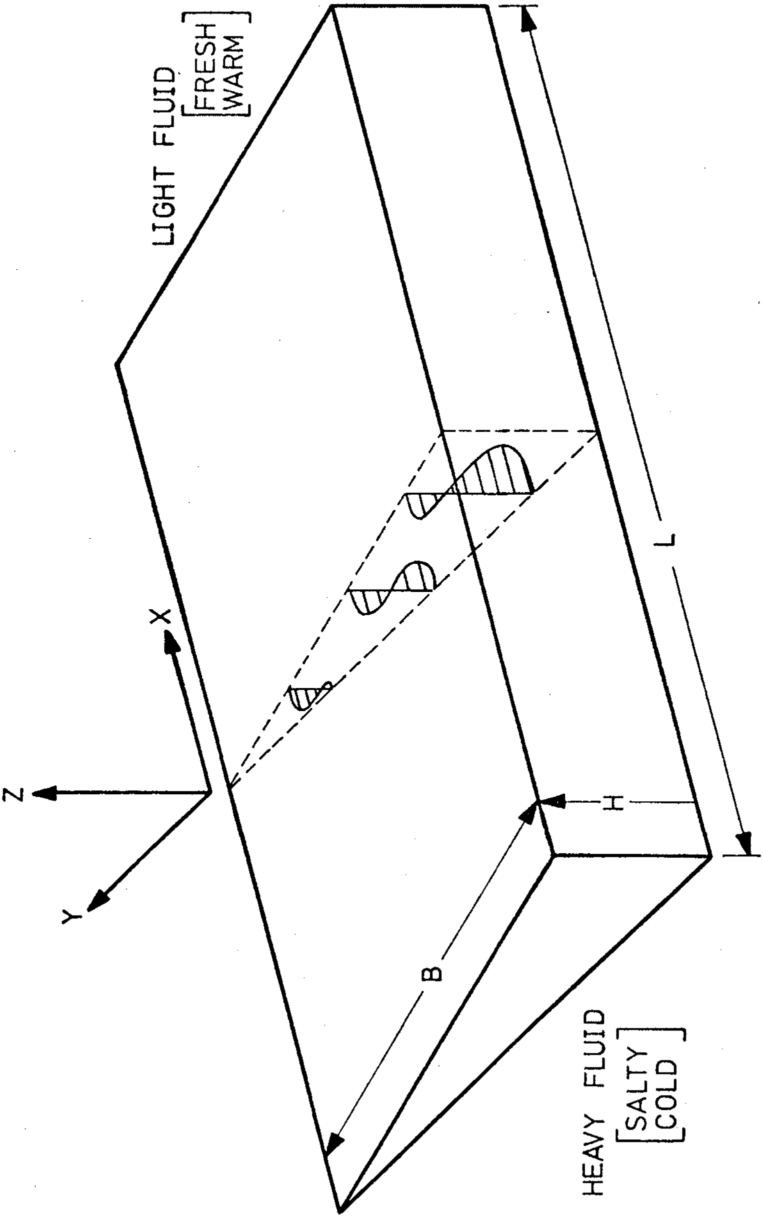

MODEL

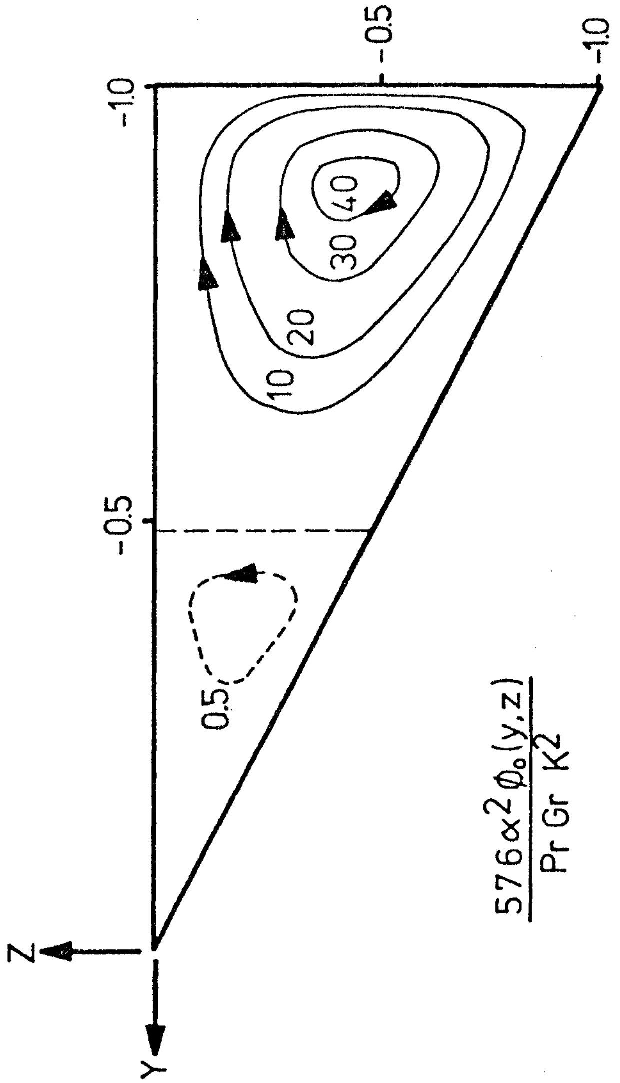
-0.5
-1.0
-1.0
-0.5
40
30
20
10
0.5
Z
Y
$\frac{576\alpha^2\phi_o(y,z)}{Pr\ Gr\ K^2}$

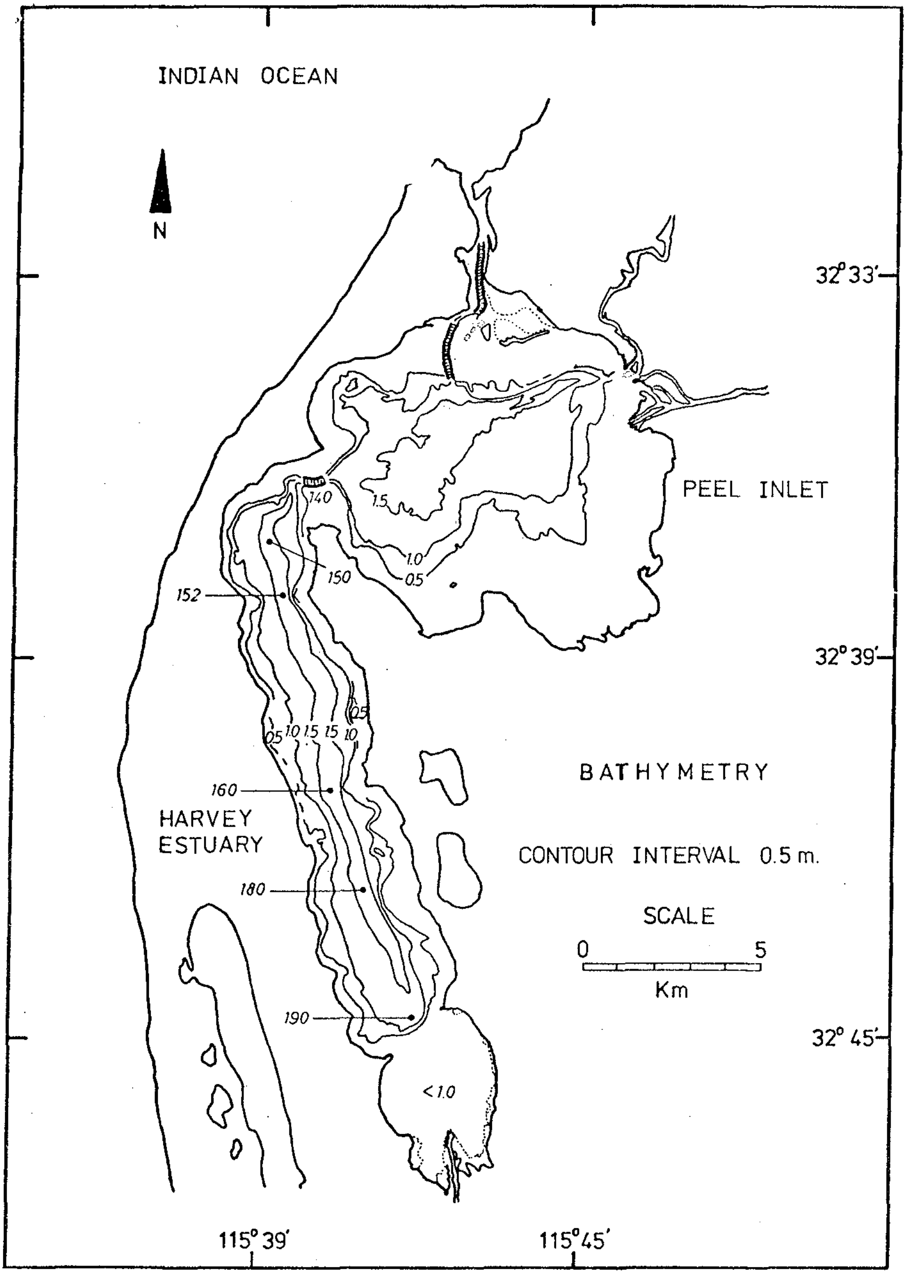
INDIAN OCEAN
N
32° 33'
32° 39'
32° 45'
PEEL INLET
HARVEY ESTUARY
BATHYMETRY
CONTOUR INTERVAL 0.5 m.
SCALE
0
5
Km
140
150
152
160
180
190
1.5
1.0
0.5
<1.0
115° 39'
115° 45'

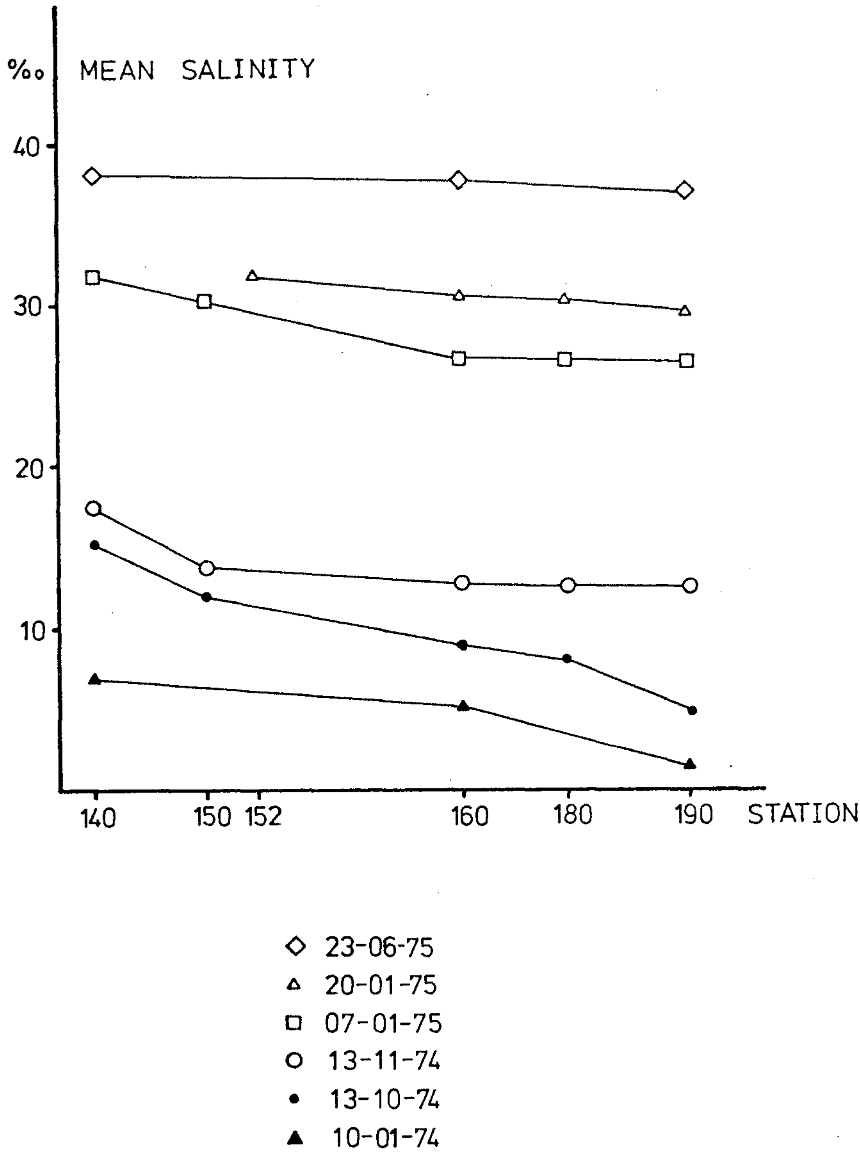
‰
MEAN SALINITY
40
30
20
10
140
150
152
160
180
190
STATION
◇ 23-06-75
△ 20-01-75
□ 07-01-75
○ 13-11-74
• 13-10-74
▲ 10-01-74